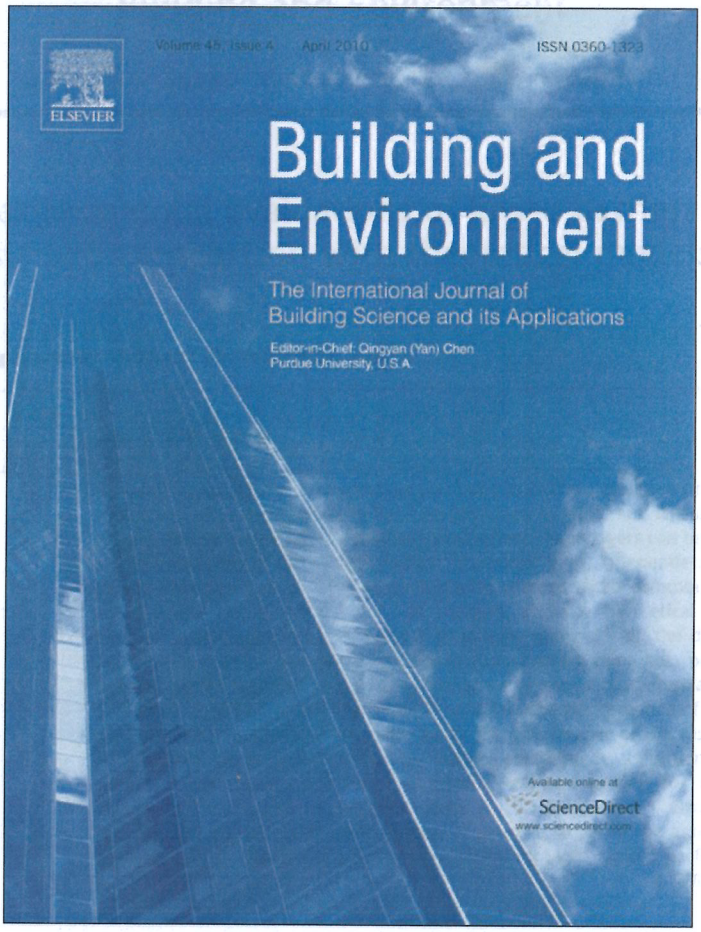

Building and Environment 44 (2009) 1107–1118

Contents lists available at ScienceDirect

Building and Environment

journal homepage: www.elsevier.com/locate/buildenv

Double skin façades for warm climate regions: Analysis of a solution with an integrated movable shading system

G. Baldinelli*

Department of Industrial Engineering, University of Perugia, Via Duranti, 67, Perugia 06125, Italy

ARTICLE INFO

Article history:
Received 7 April 2008
Received in revised form 31 July 2008
Accepted 5 August 2008

Keywords:
Double skin façade
Shading devices
Spectral optical model
Building thermal performance
Computational fluid dynamics

ABSTRACT

The analysis of a glass double skin façade equipped with integrated movable shading devices is presented, employing three different modelling levels: optics of materials, fluid dynamics of the double skin façade and building energy balance; the aim is to optimize both winter and summer energy performance. The model is developed for a façade oriented towards the south and taking into account the climatic data of central Italy; the solar radiation path with its multiple reflections at the different interfaces have been taken into account employing a ray tracing method. Simulations have been validated by the comparison with data of a similar experimental apparatus and they show that the winter configuration of the proposed façade allows a satisfactory solar heat gain in spite of the presence of shading systems. In summer, the solar heat is mainly absorbed by the external part, and even if a natural convection occurs, there is no significant influence on the inner skin and on the internal environment, thus reducing building cooling requirements. The façade performance was compared with traditional enclosures such as glazed and opaque walls in an office room in central Italy, showing that in the entire year the façade proposed significantly improves the building energy behavior, especially compared to opaque walls and when the configuration with air recovery is considered.

1. Introduction

The need to reduce energy consumption in buildings is causing a new interest towards passive solar systems. The spatial interaction between the incident radiation and the energy supplied to the internal environment is developed in different ways: in direct gain passive systems, the prevailing heat contribution is given by the solar radiation that is transmitted through transparent surfaces; the indirect gain modality takes place mainly by convection, the radiative part being supplied by storage masses (such as in Trombe walls or water walls). In the insulated gain systems, a mass storage accumulates heat by radiation and convection, but there is no passage of air to the inner space, such as in greenhouses, air collectors, solar chimneys and Barra–Costantini systems.

Used since ancient times, passive solar systems can nowadays take advantage of modern technologies, selective materials and sophisticated regulating systems; among them, double skin façades prove to be extremely attractive and promising. These façades are in fact becoming an important and widespread architectural element in office buildings, as they can provide numerous advantages beyond their good aesthetics.

A double skin façade consists of an external glass surface, a shading system, a gap filled with air and an insulating double internal glazing system, sometimes integrated with opaque walls [1]. The gap is ventilated through the airflow driven by the buoyancy effect (natural convection) or by mechanical devices (forced ventilation). The heat carried to the inner rooms is the sum of the energy directly transmitted through the transparent surfaces plus the secondary emission of the inner skin and the energy gain, if any, of the ventilation air [2], the latter depends strictly on the radiation absorbed by the entire system.

During the summer months, in countries with warm climates, the double skin configuration could easily bring about gap overheating, with the consequent dramatic increase of cooling loads [3]. With the aim of overcoming this problem, a new double skin façade is developed (Fig. 1): the external layer, made of a movable integrated glass-shading device, makes it possible to take advantage of the benefits of a typical double skin façade in winter conditions while it limits cooling loads in the warm season through its shading system, at the same time avoiding the summer greenhouse effect, changing the shape to an open configuration. The components rotation is guaranteed by a hydraulic jack; the prototype in Fig. 2 is moved by a manual crank.

A detailed analysis of the new façade is carried out through an approach that combines experimental spectrophotometric campaigns

* Tel.: +39 075 585 3868; fax: +39 075 585 3697.
E-mail address: baldinelli.unipg@ciriaf.it

0360-1323/$ – see front matter © 2008 Elsevier Ltd. All rights reserved.
doi:10.1016/j.buildenv.2008.08.005

Nomenclature

a	polynomial coefficient for transmissivity angular dependence (–).
b	polynomial coefficient for reflectivity angular dependence (–).
CFD	Computational fluid dynamics (–).
D	diameter (m).
g	gravity acceleration (m/s^2).
H	transmittance (W/m^2 K).
h	adduction coefficient (W/m^2 K).
I	turbulent intensity (%).
k	turbulent kinetic energy (m^2/s^2).
l	turbulence length scale (m).
Q	heat flux per area unit (J/m^2 s).
r	direct reflectivity factor (–).
Re	Reynolds number (–).
S	relative spectral distribution of solar radiation (–).
t	direct transmissivity factor (–).
T	temperature (K).
W	solar radiation (W/m^2).
α	absorption coefficient for opaque walls (–).
β	thermal expansion coefficient (1/K).
$\Delta\lambda$	wavelength interval (m).
ϵ	dissipation rate emission (–).
Θ	angle of incidence (°).
λ	wavelength (m).
ξ	spectral reflectance (–).
ρ	density (kg/m^3)
ψ	spectral transmittance (–).

Subscripts

0	operating temperature.
1	first polynomial coefficient.
2	second polynomial coefficient.
3	third polynomial coefficient.
4	fourth polynomial coefficient.
5	fifth polynomial coefficient.
a	absorbed.
e	solar.
ext	external.
h	hydraulic.
i	incident.
int	internal.
out	exit.
ref	value for normal incidence.

for characterizing the optical properties of materials with a three-dimensional computational fluid dynamics code, validated with data gathered form an experimental apparatus, and used as a tool for simulation models that evaluate the building energy consumption.

2. Double skin façade modelling

Double skin façades represent the result of an architectural movement which pays a great deal of attention to aesthetic matters; there are also many other advantages [4] associated with this solution, such as reduction in heating and cooling consumption, night free cooling, good façade sound insulation level and higher protection against air pollution. On the other hand, some problems could arise with the installation of glazed double skin façades [4] instead of typical external walls: overheating in summer seasons; higher investment costs, reduced floor building space and additional cleaning costs.

The main topic of scientific research on double skin façades consists of the assessment of the thermal field within the air gap. Different models have been proposed, starting from a non-dimensional analysis that introduces 14 non-dimensional numbers to describe the total heat transfer process in a naturally ventilated façade, without modelling fluid flows and heat transfer and using simple correlations to get thermal and physical data [5]. Other authors [6] suggested that in winter the air extracted by the gap could be sent to an air treatment unit as a preheated ventilation flow, thus saving a considerable amount of energy.

Deeper investigations on flow regimes between the two skins began to employ computational fluid dynamic techniques and compared the results with correlations based mainly on experimental results. In a compared study of the heat transfer by natural convection in closed rectangular vertical cavities of buildings [7], a good agreement between the CFD simulations and the data obtained by empirical correlations was found. These results enlarged the possibilities of code applications to more complex cases of façade elements, where less or even no experimental data are available in literature. What's more, it showed that errors were negligible when using three-dimensional modelling instead of restricting the

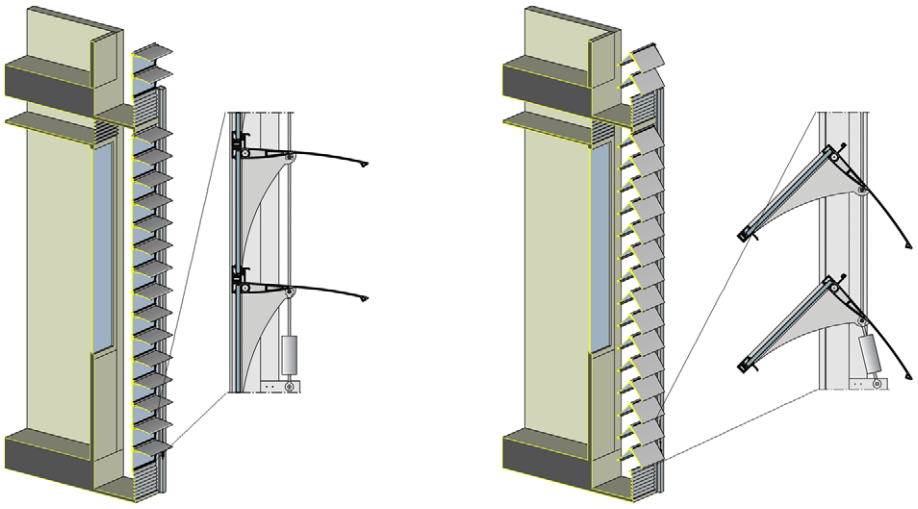

Fig. 1. Double skin façade investigated in winter and summer configurations.

Fig. 2. Prototype of the double skin façade proposed in an open configuration.

simulations to any vertical section of the façade, hypothesizing that, except for the two vertical skins, all walls are adiabatic.

A subsequent work by the same author [8] underlined that the thermal behavior of a double skin façade can be reliably described using a spectral optical model in conjunction with a CFD model including convection, conduction and radiation. The complete description of the double skin façade requires the development of three different modelling levels: optics of materials, fluid dynamics of the double skin façade and the building energy balance [9]: this approach was chosen to investigate characteristics of the façade proposed in the present study.

Particular attention has also been given to shading systems: different solutions were proposed from louvers and Venetian blinds to the "natural solution" where the gap of the double skin façade is equipped with plants [10]. If the solar shading device is positioned inside the gap, it is protected from atmospheric agents, but it modifies the airflow into the channel and becomes a heat absorber in summer, increasing the possibility of raising cooling loads [11]. External Venetian blinds, on the other hand, are in direct touch with external air, wind, rain and pollutants, but they provide better protection from incident solar heat.

Dealing with fire hazard assessment [12], some experimental investigations indicated that the gap depth is the key factor: wider gaps are safer, as well as a horizontal partition of the façade, and small tempered glass panels perform better than larger sheets because of their higher resistance to thermal stress.

3. The proposed façade

The analyzed solution [13] consists of an external layer made of an integrated glass-shading device system, making it possible to take advantage of the benefits of double skin façades in winter conditions as well as the cooling load reduction derived from the shading system in summer. When the building is located in the northern hemisphere (the opposite occurs in the southern hemisphere), the system is effective if the façade has a southern exposure.

The external skin (Fig. 2) is bounded by a stratified glass (two layers of 5-mm float glass divided by a 0.37-mm film of polyvinyl butyral) coupled with a shading device made of anodized aluminium, an alloy that combines good mechanical resistance properties with a relatively low density and an excellent performance against atmospheric agents. The inner skin should be glazed or opaque; the investigated solution is made up of transparent surfaces assembled with the coupling of the same laminated glass used for the external layer plus 4-mm float glass; the two panes are divided by a 10-mm air gap.

During wintertime shading systems are horizontal: a large amount of solar radiation can pass through the façade because the low height of the sun above the horizon allows a direct gain, together with an indirect contribution linked to multiple reflections of the opaque surface constituting the shading system. A map of the visible solar radiation absorbed by transparent surfaces of the double skin façades is plotted in Fig. 3, referring to the 15th of January, at 12:00 for a city in central Italy.

In the warm season, to avoid overheating and discomfort, the external layer remains open, allowing air to escape from the gap, thus avoiding an undesirable overheating effect, typical of double skin façades with a fixed configuration; the shading devices are configured with a high tilt angle, stopping the solar radiation. A map of the visible solar radiation absorbed by the façade is presented in Fig. 4, referring to the 15th of July, at 12:00 for the same city analyzed in wintertime.

During the cold season, the proposed façade could be set up in three configurations:

1 *open natural convection* (Fig. 5): air moves through the cavity because of buoyancy effects, the air inlet is in the lower part of the outer skin; the upper opening provides an outlet for the airflow. This layout supplies further thermal resistance between the internal and external environment compared to traditional enclosures and it makes it possible to open inner skin windows in all weather conditions, thus making natural ventilation possible;

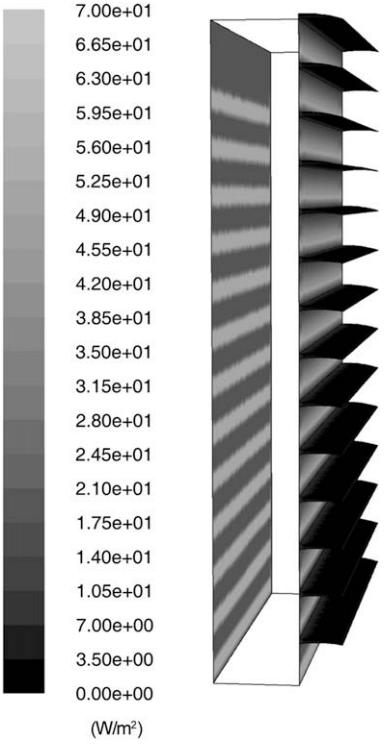

Fig. 3. Visible solar radiation absorbed (W/m^2) by transparent surfaces of the façade in winter configuration (January 15th, 12:00, central Italy).

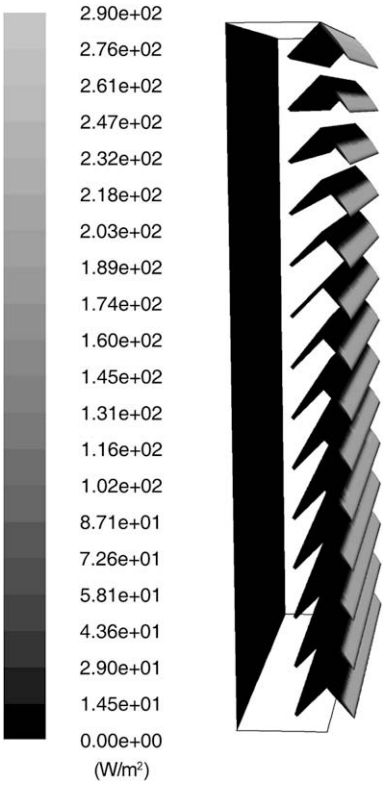

Fig. 4. Visible solar radiation absorbed (W/m^2) by the façade in summer configuration (July 15th, 12:00, central Italy).

2 *closed natural convection* (Fig. 6): this configuration also works by natural convection, but the air remains blocked in the gap where the motion starts with the characteristics of the convective motion of the air between two walls with different heat fluxes. The air in close contact with the internal environment receives more energy (both from the sun's radiation and the heat from the inner rooms) than the fluid that touches the outer skin; therefore an upper flow occurs along the hotter

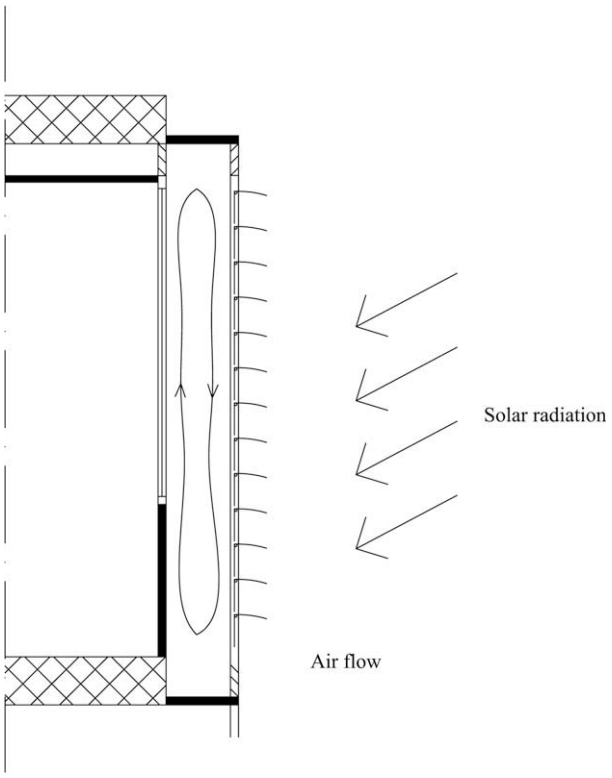

Fig. 6. Façade configuration in the heating season: closed natural convection.

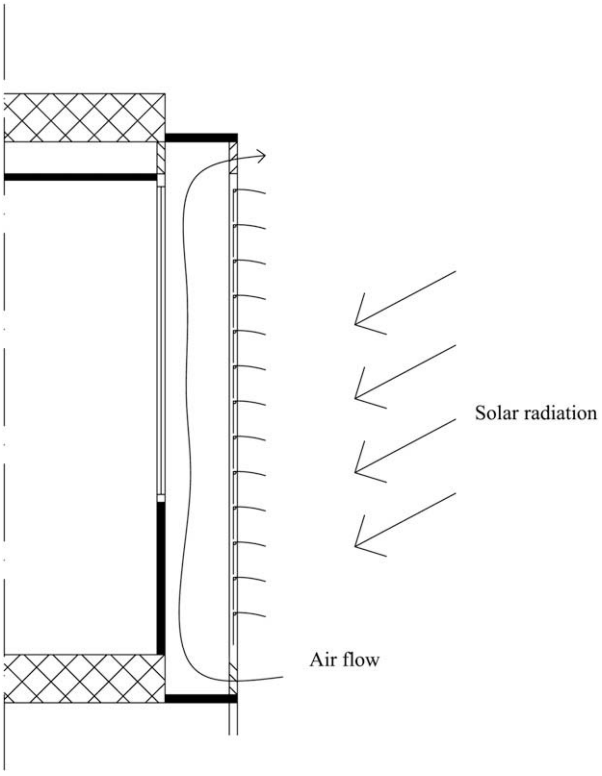

Fig. 5. Façade configuration in the heating season: open natural convection.

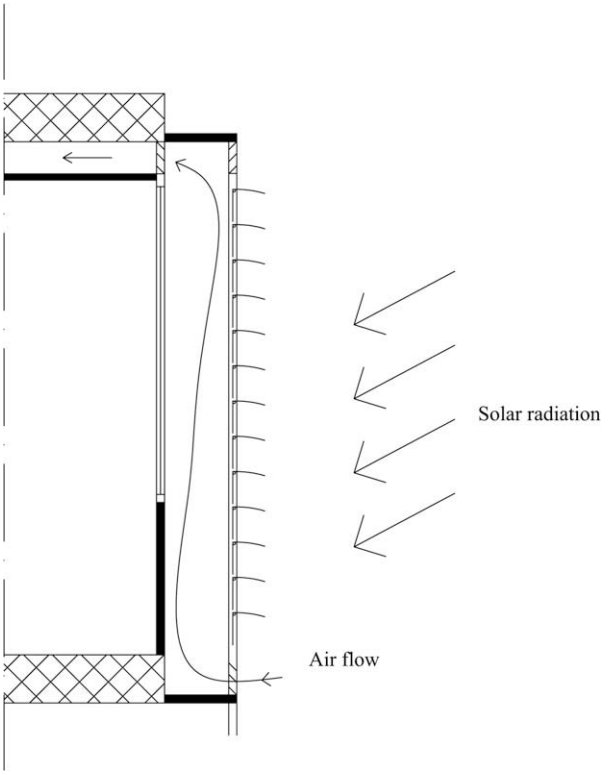

Fig. 7. Façade configuration in the heating season: forced convection.

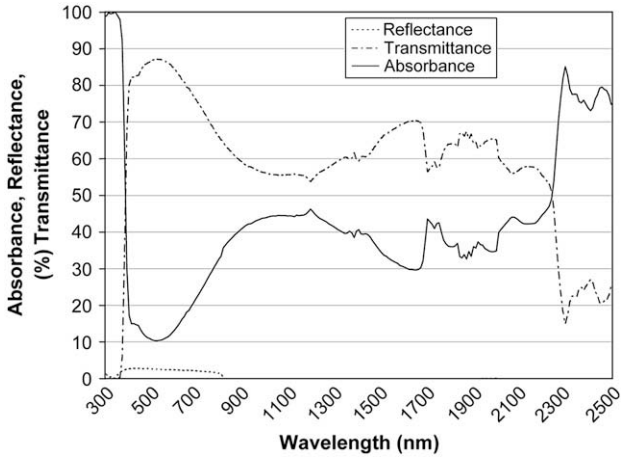

Fig. 8. Optical properties of the external skin (stratified glass).

surface while the air flows down near the colder skin. The presence of the air buffer in the gap enhances the insulating properties of the wall, but the advantage of creating natural ventilation is lost because even if the inner windows are open, the external air is not allowed to enter;

3 *forced convection* (Fig. 7): the air that circulates inside the gap is moved by a fan and sent to the inner rooms as preheated air: the air mass flow is regulated by the air conditioning system, according to ventilation requirements. This is the main energy contribution of this layout, together with the limited increase in the thermal resistance of the air gap, which is warmer than the external air.

The airflow by buoyancy or by forced convection is generally influenced by the effect of the wind that could raise or diminish significantly the flow generated inside the gap: a complete analysis should take into account of the possible interactions between these mechanisms. Nevertheless, it was decided to assume calm air outdoor conditions throughout the whole study because wind pressure is extremely variable and unpredictable, and the definition of only a single value makes results too strongly dependant on the particular case study.

4. Materials' spectral analysis

Spectral properties of the materials constituting the façade were measured through a Varian Cary 2300 precision spectrophotometer.

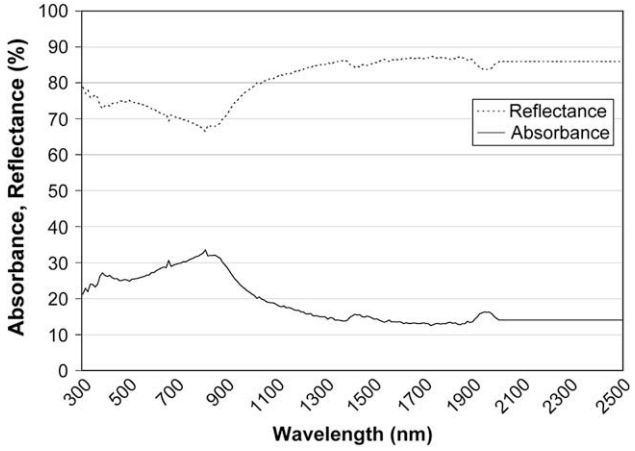

Fig. 9. Optical properties of the shading device (anodized aluminium).

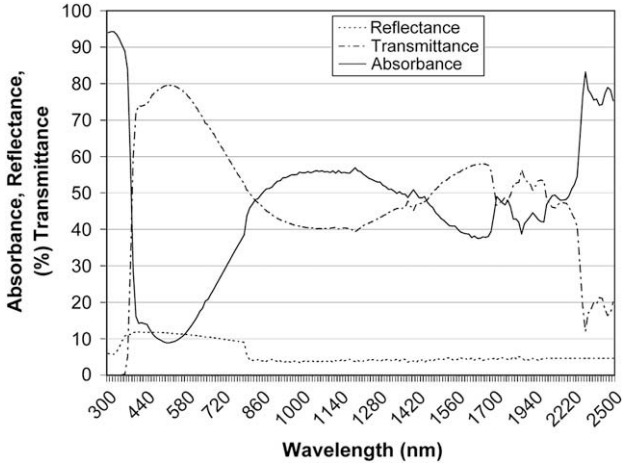

Fig. 10. Optical properties of the internal skin (stratified glass, air gap, float glass).

In Figs. 8, 9 and 10 the spectral data on the wavelength field of interest for solar radiation [14] (angular incidence, 0°) are sketched, showing the high transparency levels of both glazing systems (internal and external), as well as the good reflective properties of the aluminium in the shading system. In Table 1, results for normal incidence are reported, in terms of direct solar transmissivity factor t_e and direct solar reflectivity factor r_e, defined as follows [14]:

$$t_e = \frac{\sum_{\lambda=300\ nm}^{2500\ nm} S_\lambda \psi(\lambda) \Delta\lambda}{\sum_{\lambda=300\ nm}^{2500\ nm} S_\lambda \Delta\lambda} \quad (1)$$

$$r_e = \frac{\sum_{\lambda=300\ nm}^{2500\ nm} S_\lambda \xi(\lambda) \Delta\lambda}{\sum_{\lambda=300\ nm}^{2500\ nm} S_\lambda \Delta\lambda} \quad (2)$$

where S_λ is the relative spectral distribution of solar radiation, while $\psi(\lambda)$ and $\xi(\lambda)$ represent, respectively, the material spectral transmittance and spectral reflectance.

Glazing optical properties depend on the incident angle between the surface and the ray direction: as this angle deviates from the normal direction (0°), transmissivity decreases, reflectivity increases, and absorptivity increases.

The variation of optical properties with the incidence angle depends on glass type and thickness; in particular, it is more pronounced for multiple-pane glazing systems. In the case under investigation, the spectral transmissivity at any incident angle Θ is calculated from the normal angle of incidence, through the following relation [15]:

$$t(\Theta, \lambda) = t(0, \lambda) t_{ref}(\Theta) \quad (3)$$

Table 1
Single number optical properties of materials used for the proposed double skin façade

	External skin (laminated glass)	Shading device (anodized aluminium)	Internal skin (laminated glass, air gap, float glass)
Direct solar transmissivity factor t_e	0.69	0.00	0.58
Direct solar reflectivity factor r_e	0.01	0.75	0.11

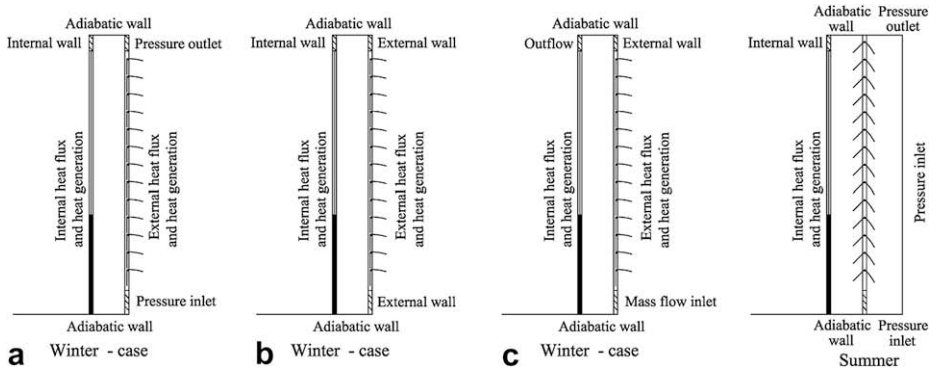

Fig. 11. Definition of boundary conditions for winter open natural convection (a), winter closed natural convection (b), winter forced convection (c) and summer.

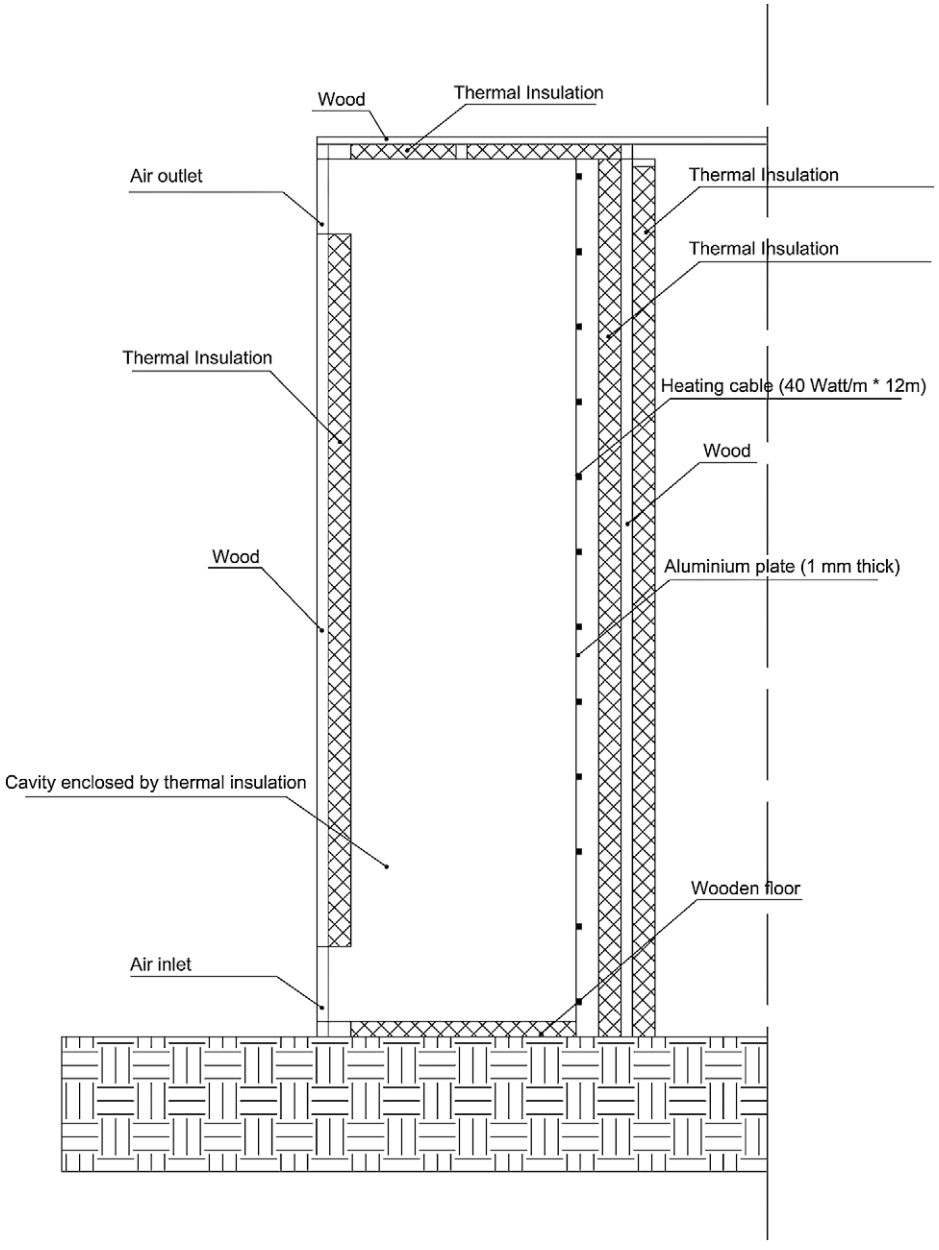

Fig. 12. Experimental apparatus used for the CFD code validation.

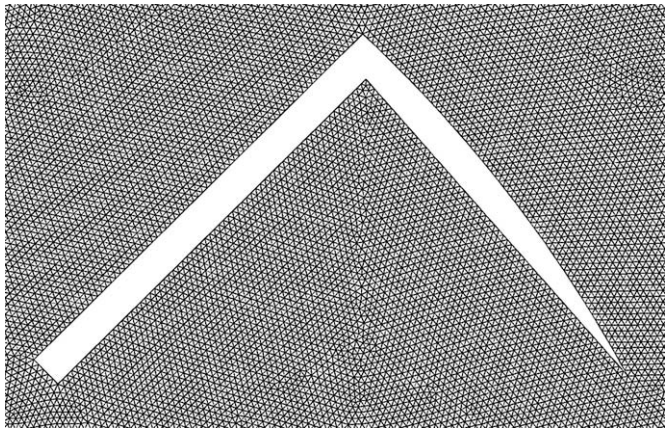

Fig. 13. Particular of the discretization mesh.

where

$$t_{\mathrm{ref}}(\Theta) = a_1 + a_2\cos\Theta + a_3\cos^2\Theta + a_4\cos^3\Theta + a_5\cos^4\Theta \quad (4)$$

similarly, the reflectivity is given by Eq. (5):

$$r(\Theta,\lambda) = r(0,\lambda)\left(1 - r_{\mathrm{ref}}(\Theta)\right) + r_{\mathrm{ref}}(\Theta) \quad (5)$$

where

$$r_{\mathrm{ref}}(\Theta) = b_1 + b_2\cos\Theta + b_3\cos^2\Theta + b_4\cos^3\Theta + b_5\cos^4\Theta \quad (6)$$

Coefficients a_i and b_i represent the polynomial coefficients for calculation of reference angular functions for coated glazings, as proposed in [15]. This approximation was chosen because it showed a good agreement with the spectrophotometric campaign conducted on the glasses used in the proposed façade: the measurement at various angles of incidence (15°, 30°, 45°, 60° and 75°) showed a difference of less than 3% from values proposed by the polynomial approximation.

Finally, to properly simulate multiple reflections occurring wherever there is a passage between two different means (e.g. air-glass), a ray tracing algorithm is employed; the model is available in the computational CFD code [16] used for the fluid dynamic analysis.

5. Numerical analysis

With the hypothesis of free convection and neglecting the effect of the wind, the flow is driven by buoyancy forces; this phenomenon is described by equations of mass, momentum and energy conservation, together with the definition of turbulent flow variables.

The time averaged momentum equation is written starting from the Reynolds form, enriched by an additional term derived by the traditional Boussinesq approximation [17], representing the coupling between temperature gradients and velocity in natural convection. This model treats density as a constant value in all solved equations, except for the buoyancy term in the momentum equation:

$$(\rho - \rho_0)g \approx -\rho_0\beta(T - T_0)g \quad (7)$$

where ρ_0 is the (constant) density of the flow at the operating temperature T_0 and β is the thermal expansion coefficient.

The code provides a solar load model that can be used to calculate the radiation effects of solar rays entering the computational domain. Since the solar ray tracing model is only available in a three-dimensional environment, the first simulations were

Table 2
Results of the validation process in terms of air volumetric flow rate comparison between the experimental data, three-dimensional and two-dimensional simulations

Gap depth (m)	Velocity flow rate (m^3/s)														
	Heat flux: 50 W/m^2					Heat flux: 110 W/m^2					Heat flux: 200 W/m^2				
	Experiment	CFD 3D	Difference (%)	CFD 2D	Difference (%)	Experiment	CFD 3D	Difference (%)	CFD 2D	Difference (%)	Experiment	CFD 3D	Difference (%)	CFD 2D	Difference (%)
0.300	0.042	0.041	−3.7	0.040	−5.0	0.054	0.052	−3.8	0.051	−5.9	0.067	0.066	−1.5	0.065	−3.1
0.500	0.040	0.041	2.4	0.040	−1.3	0.055	0.054	−1.9	0.053	−3.8	0.074	0.072	−2.8	0.071	−4.2
0.700	0.045	0.044	−3.4	0.043	−4.7	0.054	0.052	−3.8	0.051	−5.9	0.071	0.073	2.7	0.070	−1.4

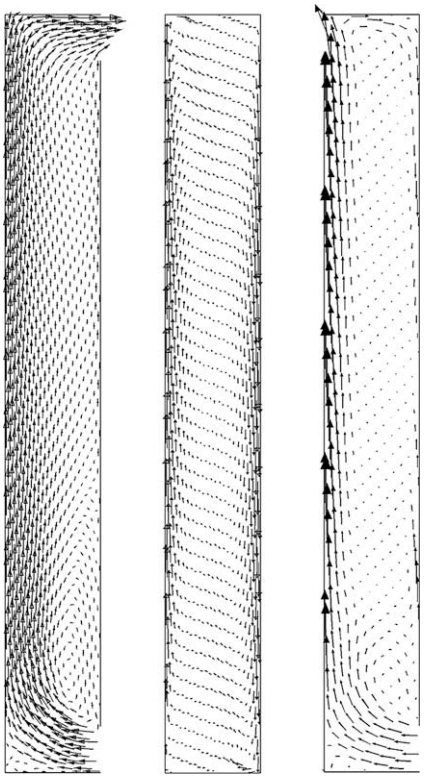

Fig. 14. Velocity vectors for open natural convection, closed natural convection and forced convection (January 15th, 12:00, central Italy).

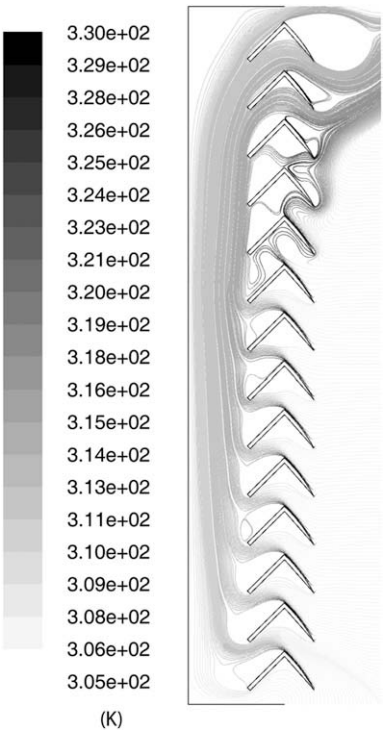

Fig. 16. Temperature air streamlines (K) in summer configuration (July 15th, 12:00, central Italy).

conducted without simplifications, with the purpose of evaluating the sun irradiation on the surfaces involved in the heat exchange (Figs. 3 and 4), considering their wavelength dependent properties obtained by the spectrophotometric campaign. The sun positions during the day and in different days of the year were obtained considering a south-oriented façade and employing geographical coordinates of the location considered, together with the Italian standard data [18] for solar irradiation.

The other boundary conditions (Fig. 11) for the winter configuration can be summarized as follows: the external wall is exchanging heat with a convection coefficient $h_{ext} = 25.0\ W/m^2\ K$; this value is arbitrarily chosen, but, at the aim of making a comparison with other façades (opaque or glazed), it was assumed the value fixed by the European standards for building

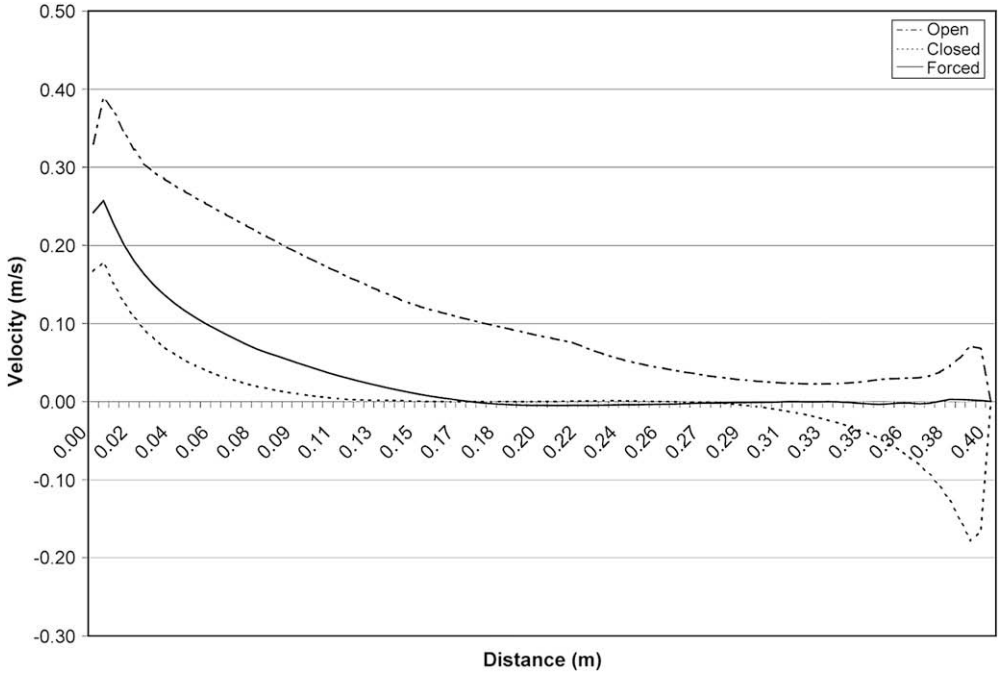

Fig. 15. Upward vertical speed for the three configurations in the middle height section (1.6 m) of the double skin façade proposed (January 15th, 12:00, central Italy).

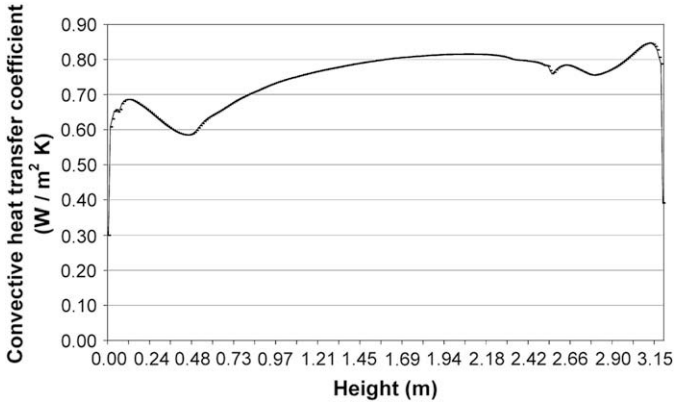

Fig. 17. Convective heat transfer coefficient on the vertical inner surface of the double skin façade.

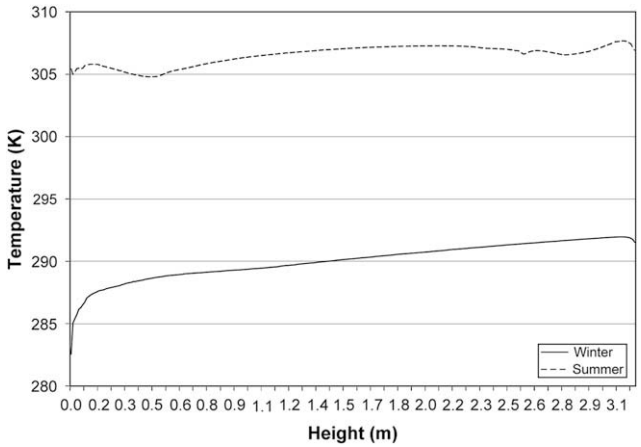

Fig. 18. Temperatures of the double skin façade vertical inner surface during the worst winter and summer conditions.

design [19]. The external temperature is a function of the time of the day and the site: its values for each simulation were set according to the same Italian standard data used for solar irradiation. Focusing attention on the indoor heat exchange, it is assumed that inner rooms remain at 293 K, while the internal convection coefficient is considered to be $h_{int} = 7.7$ W/m^2 K, choosing again the same value reported in the abovementioned European Standard. The upper and lateral walls are considered adiabatic and they do not participate in the solar ray tracing; when an open natural configuration (a) is studied, the bottom opening is given a pressure inlet boundary condition (101,325 Pa) with the turbulent intensity I and the turbulence length scale l equal to 6 % and 0.025 m, respectively. The choice of these values derives from the equations that define the two quantities in terms of the Reynolds number and the hydraulic diameter [20]:

$$I = 0.16 Re_{D_h}^{-1/8} \tag{8}$$

$$l = 0.07 D_h \tag{9}$$

The external upper opening is given pressure outlet boundary conditions with the same turbulent quantities values, while the other upper opening is considered as an internal wall. In the closed natural convection configuration (b), all the openings are considered as walls, whereas with forced convection (c), in the lower opening the mass flow rate is fixed, imposing an outflow condition in the inner upper opening, and leaving the external upper opening as a wall. Boundary conditions for the open configuration (summer) differ only for the external skin, which is no longer a wall, but is entirely in direct contact with the external air. The dominion is extended, including a part of the external environment and giving pressure inlet and outlet conditions to the border surfaces (Fig. 11); the inner upper opening remains as a wall.

6. CFD validation process

After the definition of the simulation tool, an accurate validation process has been conducted, selecting the most complex configuration of the double skin façade: the open natural convection, described in paragraph 3. This choice was dictated by the consideration that, with natural convection, models representing air motion inside the gap are rather complex, involving turbulent and laminar flows, as well as recirculation phenomena and the intrinsic difficulty in defining the type of flow (laminar or turbulent). Therefore, once the CFD tool is validated for this type of flow regime, it is reasonable to expect that results for the other two configurations could be considered reliable.

Data used for the validation have been taken from a study realized by Yin-Hao Chiu and Li Shao [21] in the Institute of Building Technology of Nottingham University; the aim of this experimental campaign consisted of investigating the influence of solar heat flux and geometric parameters on a double skin façade thermal performance. The analysis was conducted on a three-dimensional model made of two opaque walls with an inlet (bottom) and outlet (top) opening in the external wall and where a buoyancy driven flow regime was established; the experimental apparatus is shown in Fig. 12.

Except for the inner and outer skin, all the other surfaces were considered adiabatic and the effect of the solar radiation was substituted by an aluminium heating cable positioned near the inner wall.

Moving to the CFD model definition, the renormalisation group k–ϵ model was chosen to simulate the air motion inside the double skin façade cavity, as suggested in [22]; besides, the wall effect on the air motion has been taken into account using a fine near-wall mesh or, reducing computational requirements, introducing the enhanced wall treatment: a near-wall modelling method that combines a two-layer model with enhanced wall functions. This was the solution adopted; in Fig. 13 a particular of the discretization mesh is reported, referring to the summer configuration.

In Table 2 a comparison between results obtained from experimental data and simulations are reported in terms of air volumetric flow rate; in the same table the values of the flow rate obtained by a two-dimensional approach are also reported: it is shown that numerical analysis data bring to errors that never exceed 6% respect to the measured values. The three-dimensional simulations reveal more accurate: from the two-dimensional model a light underestimation of the flow rate emerges; this is probably due to the fact that the edge effect of the adiabatic lateral walls of the three-dimensional model keeps the fluid warmer, so favouring natural convection. Nevertheless, the two-dimensional simulations give an almost negligible additional error; therefore, the fluid dynamics analysis of the entire validation phase and the study of the proposed façade was developed with the two-dimensional configuration.

Finally, a grid independence check was done through a series of grid refinements and the optimal size for the two-dimensional approach was found for a grid of around 125,000 cells; each further refinement gave a difference of less than 1% on the main thermodynamic parameters.

Table 3
Energy comparison (heat gain) between the double skin façade proposed (forced convection), a glazed wall, an opaque wall and a mix of them for winter season

Month	Double skin façade				Glazed wall			Opaque	Daylight hours	Heating days	Double skin façade total gain (kWh/m² month)	Glazed façade total gain (kWh/m² month)	Opaque façade total gain (kWh/m² month)	Mixed façade total gain (kWh/m² month)
	Wall heat flux (W/m²)	Solar direct transmission (W/m²)	Air preheating (W/m²)	Total heat flux (W/m²)	Solar direct transmission (W/m²)	Wall heat flux (W/m²)	Total heat flux (W/m²)	Total heat flux (W/m²)						
October	15.3	41.1	21.7	78.0	187.8	0.0	187.8	1.0	11	17	11.8	32.3	−0.3	11.8
November	16.1	58.0	32.4	106.5	165.8	−11.8	154.0	−1.0	9	30	18.5	31.3	−1.9	18.5
December	8.8	55.6	35.9	100.3	126.9	−22.9	104.1	−3.0	9	31	13.4	14.5	−3.1	13.4
January	7.8	57.1	39.4	104.3	153.1	−24.4	128.7	−3.1	9	31	13.1	19.9	−3.4	13.1
February	−6.1	23.8	27.0	44.7	139.5	−21.7	117.9	−2.8	10	28	−0.1	20.3	−2.8	−0.1
March	−7.8	11.7	19.3	23.2	129.5	−16.6	112.9	−1.9	12	31	−0.9	32.4	−2.2	−0.9
April	−3.8	10.7	14.8	21.7	104.3	−10.8	93.6	−1.1	13	15	1.2	15.2	−0.7	1.2
Total (kWh/m² year)											56.9	166.0	−14.3	75.8

7. Effects on building energy consumption: comparison with standard walls

The knowledge of the thermodynamic behavior of the proposed façade constitutes the basis for the energy analysis of buildings equipped with this solution. The investigation was conducted in a city in central Italy for an office building with the double skin façade exposed towards the south direction. The entire year was considered, taking into account the heating season for the place considered (October 15th to April 15th) while the summer season was circumscribed to the months of June, July, August and September.

The results of the CFD analysis for the three winter configurations are shown in Fig. 14, referring to the 15th of January. The air mass flow rate in forced convection was fixed in 0.017 kg/s, according to ventilation requirements for offices defined in the Italian Standard [23] and hypothesizing that each façade frontal linear meter supplies 10 internal square meters. The upward vertical component of velocity in the horizontal section at half height (1.6 m) of the façade is plotted in Fig. 15; it is showed that the highest velocities in each configuration are reached near the left wall, because of the contemporary presence of the heat flux from inner rooms and the solar flux from transparent surfaces. In the closed configuration, the instauration of a convective flow creates a downward stream near the right (external) wall.

In Fig. 16, the temperature streamlines referring to one of the hottest days of the year (July 15th, with an external temperature of 307 K) show how the solar heat is mainly absorbed by the external part and a natural convection occurs, without influencing significantly the inner skin and the internal environment. In fact, it can be seen how the air that laps the inner wall has temperatures close to the air temperature coming from outside (around 307 K). Besides, as plotted in Fig. 17, the convective heat transfer coefficient on the double skin façade inner surface is never higher than 1 W/m² K. Therefore, in summer, the only amount of cooling load entering by radiation through transparent surfaces is considered, since the heat entering the building by convection results negligible.

The energy behavior of the proposed double skin façade was tested comparing its performance with a wall made of an opaque surface, a glazed wall, and a mix of them (50% opaque surface and 50% glazed surface). Each wall meets the requirements of the recent Italian Legislative Decree no. 311 [24] on energy saving in buildings.

In wintertime, when the sun is absent, the energy lost through any surface is linked to the wall transmittance, as well as to the temperature difference between the inner rooms (293 K) and the external environment (average monthly temperature as defined in [18]). When the sun appears, different solar gains emerge for each enclosure:

- *double skin façade*: a part of solar radiation is directly transmitted to the inner rooms, according to the glazing transmissivity, with a significant reduction due to the shading effect of the opaque surfaces. Another part of solar radiation is absorbed by the inner skin and by the air in the gap: the resulting effect is the temperature raising of the internal wall (T_{wall}), thus reducing the heat flux to the following value:

$$Q_{out} = h_{int}{}^{*}(T_{int} - T_{wall}) \quad (10)$$

In the forced convection configuration, the contribution of air preheating adds to the solar heat gains:

- *glazed wall*: the same phenomena described for the double skin façade remain valid for a glazed wall; the direct transmission is obviously increased (the shading systems are absent) while the contribution of air heating is lacking;

Table 4
Energy comparison (cooling load entering the building) between the double skin façade proposed, a glazed wall, an opaque wall and a mix of them for summer season

Month	Double skin façade			Glazed wall			Opaque	Daylight hours	Cooling days	Double skin façade total load (kWh/m² month)	Glazed façade total load (kWh/m² month)	Opaque façade total load (kWh/m² month)	Mix façade total load (kWh/m² month)
	Solar direct transmission (W/m²)	Wall heat flux (W/m²)	Total heat flux (W/m²)	Solar direct transmission (W/m²)	Wall heat flux (W/m²)	Total heat flux (W/m²)	Total heat flux (W/m²)						
June	3.9	0.0	3.9	61.7	5.6	67.3	1.5	15	30	1.8	30.4	0.7	15.5
July	4.4	0.0	4.4	65.5	6.2	71.7	1.6	14	31	4.0	33.2	0.7	16.9
August	4.1	0.0	4.1	91.0	8.4	99.4	2.1	13	31	3.6	42.1	0.8	21.4
September	3.4	0.0	3.4	116.8	10.4	127.2	2.5	12	30	0.9	45.5	0.9	23.2
Total (kWh/m² year)										10.3	151.1	3.1	77.1

Table 5
Energy comparison (total saving) between the three configurations of the double skin façade proposed, a glazed wall, an opaque wall and a mix of them for the entire year

	Double skin façade (forced convection)	Double skin façade (closed convection)	Double skin façade (natural convection)	Glazed façade	Opaque façade	Mix façade
Winter solar heat gain (kWh/m^2 year)	56.9	22.7	2.8	166.0	−14.3	75.8
Summer cooling load (kWh/m^2 year)	10.3	10.3	10.3	151.1	3.1	77.1
Total saving (kWh/m^2 year)	46.6	12.4	−7.5	14.9	−17.4	−1.3

- *opaque surface*: there is no direct transmission, the only contribution is due to the radiation absorbed by the wall [25] which, disregarding the losses by radiation, is written as follows:

$$Q_{abs} = \frac{W_i \ \alpha \ H}{h_{ext}} \tag{11}$$

where H is the wall transmittance, W_i is the solar incident power, h_{ext} is the external convection coefficient and α is the absorption coefficient of the outer surface: 0.6 for a medium color (neither dark nor light) surface.

In the warm season, on the contrary, the solar radiation intensifies the necessity of heat removal; therefore, values calculated as solar gains in winter become the cooling load in summer.

Fig. 18 shows the wall temperature on the inner surface (glass) in correspondence to the worst winter and summer conditions: the external temperatures are equal to 277 K and 307 K; respectively, it is showed how the glass surface temperature becomes closer to inner rooms air values. Beyond the beneficial effect on energy savings, the consequence consists also of an improvement of indoor conditions. In fact, external transparent walls are often the surfaces with the higher specific heat exchange rate by radiation, being strongly influenced by the external environment; the double skin façade smoothes the internal mean radiant temperature, so enhancing comfort conditions.

The glazed surface was assumed to be equipped with an inner white curtain, with a shading coefficient equal to 0.8, according to EN 832. The energy analysis considered the total heat gain from the façade in the cold season (energy saving on the HVAC system) as well as the cooling energy necessary to remove the solar radiation that enters the building (energy demand on the HVAC system). The considered office has a square plan with a width of 10.0 m size and a height of 3.2 m [26]; one side (the one face facing south) constituted the analyzed façade, which, therefore, has a total surface area of 32.0 m^2. The monthly evaluation of the normalized (per square meter) energy exchanges is done referring to the 15th day, considered representative of the entire month; the analysis is, therefore, conducted taking into account only of heat fluxes through the façade and energy necessary for indoor ventilation requirements [23].

Tables 3 and 4 show an example of the compared analysis results, for winter and summer conditions; respectively, the double skin façade configuration is the forced convection one. During the cold season (from October to April) negative total heat gains may rise sometimes from the façade; in these cases, the façade itself is not a source of energy saving but it generates a further load on the heating system to be added to other loads always present in these periods such as, for example, dispersions through other walls of the envelope.

The comparison between the three façade configurations and the other envelopes analyzed is shown in Table 5.

It is evident that the proposed solution is the most efficient of all the configurations, when the forced convection mode is activated. The performance was found to be the best of all the envelopes considered, and the difference is more pronounced compared to the opaque surfaces, where the improvement reaches up to 60 kWh per year per square meter of façade.

With the closed configuration, the performance gets poorer and it becomes similar to a one-skin glazed façade, because the contribution of air preheating is lost; in any event, the result is better than the opaque wall and the mixed solution. The open configuration is the least efficient in energy terms, because the heat given to the air by buoyancy escapes through the upper opening.

8. Conclusions

A new double skin façade with a movable integrated shading system has been investigated, defining its energy performance starting by measuring optical properties of materials and implementing a computational fluid dynamics analysis, validated by a comparison with data of a similar experimental apparatus. The study of its thermodynamic behavior showed good performance both in winter conditions as well as in the warm season, where traditional double skin façades show weak performance because of gap overheating. The energy analysis pointed out the strong effect of the spectral properties of each component: the high reflection shading devices allow a satisfactory solar gain in winter and a considerable cooling load reduction in summer.

The simulation of façade performances with a CFD model for the winter configuration (shading closed) showed the instauration of a buoyancy induced flow inside the gap, producing the doubly beneficial effect of diminishing the heat dispersion through external walls and preheating the air for ventilation purposes. Summer simulations show good system behavior due to the contributions of the high shading level and the open configuration that inhibits overheating, one of the main obstacles to the use of double skin façades in warm climate countries.

The façade performance was compared with traditional enclosures such as glazed and opaque walls in an office room in central Italy; results showed that in the entire year the façade proposed significantly improves the building energy behavior, especially when the configuration with winter forced convection is considered. In this case, in fact, the joint contribution of air preheating and gap thermal resistance enhancement makes the performance of the double skin façade particularly interesting: the comparison with opaque walls showed an energy saving up to 60 kWh per year per façade square meter. When differences with a standard glazed surface solution are analyzed, energy improvements result weakened, but the indoor comfort improves significantly because of smoother mean radiant temperature.

The movable configuration of the façade proposed implies a detailed design case by case and a higher investment costs, making difficult a wide and quick diffusion; besides, additive maintenance matters have to be taken into account, especially if the motion mechanism is automatic.

Difficulties deriving from the need of implementing a different project for each different building analyzed could be overcome

through the use of the simulation model proposed. On the other hand, when quick variations of external climatic parameters are found, the steady state hypothesis is no more applicable; therefore, it will be useful to extend the analysis to unsteady conditions.

Future work should deal with the extension of the analysis to different sites, with a greater number of days investigated each month and assessing the performance of the façade proposed with the variation of geometric parameters such as the shading shape and tilt. It will be also useful to analyze the effect of the façade in the natural lighting of inner rooms, since the shading system is not removable and its configuration in winter conditions is fixed.

References

[1] Wigginton M, Harris J. Intelligent skins. Oxford: Elsevier; 2002. p. 72.
[2] Infield D, Mei L, Eicker U. Thermal performance estimation for ventilated PV façades. Solar Energy 2004;76:93–8.
[3] Gratia E, De Herde A. Natural cooling strategies efficiency in an office building with a double-skin façade. Energy and Buildings 2004;36:1139–52.
[4] Poirazis H. Double skin façades for office buildings literature review. Sweden: Department of Construction and Architecture Lund University; 2004. pp. 61–66.
[5] Balocco C. A non-dimensional analysis of a ventilated double façade energy performance. Energy and Buildings 2004;36:35–40.
[6] Corgnati SP, Perino M, Serra V, Filippi M. Analisi del comportamento termo-fluidodinamico di un involucro trasparente innovativo: risultati di una campagna di monitoraggio. In: Proceedings of 58th Congress of Associazione Termotecnica Italiana. San Martino di Castrozza, Italy: ATI; 2003. p. 1457–68.
[7] Manz H. Numerical simulation of heat transfer by natural convection in cavities of façade elements. Energy and Buildings 2003;33:305–11.
[8] Manz H. Total solar energy transmittance of glass double façades with free convection. Energy and Buildings 2004;36:127–36.
[9] Manz H, Frank T. Thermal simulation of buildings with double-skin façades. Energy and Buildings 2005;37:1114–21.
[10] Stec WJ, van Paassen AHC, Maziarz A. Modelling the double skin façade with plants. Energy and Buildings 2005;37:419–27.
[11] Gratia E, De Herde A. The most efficient position of shading devices in a double-skin façade. Energy and Buildings 2007;39:364–73.
[12] Chow WK, Hung WY. Effect of cavity depth on smoke spreading of double-skin façade. Building and Environment 2006;41:970–9.
[13] Belardi P, Bianconi F, Asdrubali F. SUN-SHADE – Sistema innovativo di facciata a doppio involucro con frangisole integrato. Libria: Perugia; 2007.
[14] EN 410. Glass in building – determination of luminous and solar characteristics of glazing. European Standard, 1998.
[15] American Society of Heating, Refrigerating and Air-Conditioning Engineers Inc.. ASHRAE handbook fundamentals. SI ed. Atlanta: American Society of Heating, Refrigerating and Air-Conditioning Engineers Inc.; 2001. pp. 30.18–30.25.
[16] Fluent Version 6.2 – User's Guide. USA; 2005.
[17] Rodrigues AM, Canha da Piedade A, Lahellec A, Grandpeix JY. Modelling natural convection in a heated vertical channel for room ventilation. Building and Environment 2000;35:455–69.
[18] UNI 10349. Riscaldamento e raffrescamento degli edifici. Dati climatici. Italian Standard, 1994.
[19] ISO 6946. Building components and building elements – thermal resistance and thermal transmittance – calculation method. European Standard, 2007.
[20] Safer N, Woloszyn M, Roux JJ. Three-dimensional simulation with a CFD tool of the airflow phenomena in single floor double-skin facade equipped with a Venetian blind. Solar Energy 2005;79:193–203.
[21] Chiu Y, Shao L. An investigation into the effect of solar double skin façade with buoyancy-driven natural ventilation. In: Proceedings of the CIBSE National Conference. London, UK: CIBSE; 2001. p. 9.
[22] Gan G. Thermal transmittance of multiple glazing: computational fluid dynamics prediction. Applied Thermal Engineering 2001;21:1583–92.
[23] UNI 10339. Impianti aeraulici al fini di benessere. Generalità, classificazione e requisiti. Regole per la richiesta d'offerta, l'offerta, l'ordine e la fornitura. Italian Standard, 1995.
[24] Italian Legislative Decree n. 311. Disposizioni correttive ed integrative al decreto legislativo 19 agosto 2005, n. 192, recante attuazione della direttiva 2002/91/CE, relativa al rendimento energetico nell'edilizia. 2006.
[25] EN 832. Thermal performance of buildings – calculation of energy use for heating – residential buildings. European Standard, 1998.
[26] Todorovic B, Maric B. The influence of double facades on building heat losses and cooling loads. In: Proceedings of 20th international congress of refrigeration. Sydney, Australia: ICR; 1999.